# PROCEEDINGS

Of SPIE-The International Society for Optical Engineering

Volume 846


# Digital Image Processing and Visual Communications Technologies in Meteorology


Paul Janota
Chair/Editor



*Sponsored by*
SPIE—The International Society for Optical Engineering

27-28 October 1987
Cambridge, Massachusetts

Proceedings of SPIE—The International Society for Optical Engineering

Volume 846

# Digital Image Processing and Visual Communications Technologies in Meteorology

**Paul Janota**
*Chair/Editor*

*Sponsored by*
SPIE—The International Society for Optical Engineering

**27-28 October 1987**
**Cambridge, Massachusetts**

*Published by*
**SPIE—The International Society for Optical Engineering**
**P.O. Box 10, Bellingham, Washington 98227-0010 USA**
Telephone 206/676-3290 (Pacific Time) • Telex 46-7053

The papers appearing in this book comprise the proceedings of the meeting mentioned on the cover and title page. They reflect the authors' opinions and are published as presented and without change, in the interests of timely dissemination. Their inclusion in this publication does not necessarily constitute endorsement by the editors or by SPIE.

Please use the following format to cite material from this book:
Author(s), "Title of Paper," *Digital Image Processing and Visual Communications Technologies in Meteorology,* Paul Janota, Editor, Proc. SPIE 846, page numbers (1987).

Library of Congress Catalog Card No. 87-63192
ISBN 0-89252-881-8



Printed in the United States of America.

*DIGITAL IMAGE PROCESSING AND*
*VISUAL COMMUNICATIONS TECHNOLOGIES IN METEOROLOGY*

Volume 846

## Conference Committee

*Chair*
**Paul Janota**
The Analytic Sciences Corporation

*Cochairs*
**Edwin Catmull**
Pixar

**Mary des Jardins**
NASA/Goddard Space Flight Center

**Robert Fox**
University of Wisconsin

**Victor Tom**
Atlantic Aerospace Electronics Corporation

**Thomas H. Vonder Haar**
Colorado State University

*Session Chairs*
Session 1—Digital Image Processing of Remotely Sensed Data
**Mary des Jardins,** NASA/Goddard Space Flight Center
**Thomas H. Vonder Haar,** Colorado State University

Session 2—Visual Communication of Meteorological Phenomena
**Robert Fox,** University of Wisconsin
**Victor Tom,** Atlantic Aerospace Electronics Corporation

Session 3—Meteorological Workstation Technology
**Edwin Catmull,** Pixar

*DIGITAL IMAGE PROCESSING AND*
*VISUAL COMMUNICATIONS TECHNOLOGIES IN METEOROLOGY*

Volume 846

# INTRODUCTION

This was the first conference in this topical area sponsored by SPIE. It provided several pleasant surprises, including variety, an international flavor, and the opportunity to get well acquainted with the various participants and their areas of interest.

The first session presented in this proceedings is Digital Image Processing of Remotely Sensed Data; it primarily covers a number of automated techniques for detecting and identifying features derived from both satellite and radar imagery, plus other topics associated with satellite remote sensing. Applications of such techniques include both real-time analysis and prediction of meteorological events and monitoring of world climate.

The second session, Visual Communication of Meteorological Phenomena, focuses on the use of three- or four-dimensional renderings (on two-dimensional devices) and/or the use of color in depicting analyses, forecasts, and the output of research models. The major discussion issue of this session is whether there is added value derived from the use of the various display techniques in real-time and research modes. Some authors feel that technology has outstripped utility and that we have not yet developed the appropriate quantitative models to take full advantage of the clever visualizations that are possible at rather low cost. There seems to be general agreement, however, that a user's rapid assimilation and understanding of complex meteorological phenomena will eventually be improved by modern visualization techniques combined with appropriate algorithms and models to best complement the available technologies.

The third session, Meteorological Workstation Technology, emphasizes the architectures of certain systems rather than the information products displayed on the workstations themselves.

A straw poll of participants revealed a solid interest in continuing this conference and considerable satisfaction with the format that provided for in-depth presentations and ample time for discussion. I wish to thank my cochairs for their assistance and support, and SPIE for hosting the conference in such a professional fashion.

**Paul Janota**
The Analytic Sciences Corporation

*DIGITAL IMAGE PROCESSING AND*
*VISUAL COMMUNICATIONS TECHNOLOGIES IN ME*

Volume 846

## Contents

*DIGITAL IMAGE PROCESSING AND*
*VISUAL COMMUNICATIONS TECHNOLOGIES IN ME*

Volume 846

**Session 1**

**Digital Image Processing of Remotely Sense**

*Chairs*
**Mary des Jardins**
NASA/Goddard Space Flight Center
**Thomas H. Vonder Haar**
Colorado State University

# Classification of cloud fields based on textural

R. M. Welch, S. K. Sengupta,* and D. W.

South Dakota School of Mines and Technology, Institute o
501 E. St. Joseph Street, Rapid City, South Dako

## 1. INTRODUCTION

Textural features have been widely used by the pattern reco classification of digital images.[4,11,14] However, the meteoro virtually ignored texture-based methods in cloud classificatio upon spectral signatures[3] is at least in part due to the studi and Rosenfeld.[13] They found that attempts to resolve ambiguit type signatures by the addition of textural features did not p tion in misclassification errors. However, these results were resolution in the visible channel and 4 n mi spatial resolutio present study reexamines the applicability of texture-based fe classification using very high spatial resolution (57 m) LANDS digital data. We conclude that cloud classification can be ac single visible channel.

## 2. OVERVIEW

First and second order statistical measures of image gray l define textural features. Haralick et al.[6] used a set of 14 s upon Gray Level Cooccurrence Matrices for image classification later proposed some additional measures based on the third and second order statistics. The concept of gray level cooccurren to Generalized Cooccurrence Matrices (GCM).[5]

Viewing image texture from a different perspective, Mitchel textural measure based on the statistical properties of signif gray levels. The resulting MAX-MIN algorithm has advantages o of being hardware-implemented. Sengupta et al.[16] introduced a the analysis of local extremes of MAX-MIN and that of the GCM, joint distribution of adjacent pairs of significant local extr distances. The statistical measures derived from the generali are then viewed as the textural characteristics of the image. both the magnitude of the extrema and the distance separating images taken from Brodatz[2] were classified with 95%-97% accura

## 3. CLASSIFICATION FEATURES

The Max-Min Cooccurrence Matrix (MMCM) method first locates extremes in gray level along a horizontal scan. Here, by "sig the gray levels I,J of adjacent pairs of local-maximum-to-loca satisfy

$$|I-J|>T \quad ,$$

where T is an appropriate threshold. A value of T=1 is used i $m(I,J)_d$ be the number of adjacent local extrema with gray leve pixel distance d. For fixed d, m(I,J) is normalized to constr $P(I,J)_d$ which then is used to derive the textural measures lis is dropped for convenience).

(2) The first order statistics associated with P(I) and P(
distributions of local maxima and minima:

(a) means $\mu_x$, $\mu_y$

(b) variances $\sigma_x^2$, $\sigma_y^2$

(3) Contrast: $CONTR = \sum_{I,J} (I-J)^2 P(I,J)$

(4) Angular Second Moment: $ASM = \sum_{I,J} P(I,J)^2$

(5) Correlation: $CORR = [\sum_{I,J} IJP(I,J) - \mu_x\mu_y]/\sigma_x\sigma_y$

(6) Entropy: $ENTROPY = - \sum_{I,J} P(I,J) \log P(I,J)$

(7) Local Homogeneity: $HOMOG = \sum_{I,J} P(I,J)/[1+(I-J)^2]$

(8) Cluster Shade[19] for

(a) difference: $SHADE = \sum_{I,J} [(I-J)-(\mu_x-\mu_y)]^3 P(I,J)/[\sigma$

(b) sum: $SHADEX = \sum_{I,J} [(I+J)-(\mu_x+\mu_y)]^3 P(I,J)/(\sigma_x^2+2\sigma_{xy}$

(9) Cluster Prominence[19] for

(a) difference: $PROM = \sum_{I,J} [(I-J)-(\mu_x-\mu_y)]^4 P(I,J)/(\sigma_x^2$

(b) sum: $PROMX = \sum_{I,J} [(I+J)-(\mu_x+\mu_y)]^4 P(I,J)/(\sigma_x^2+2\sigma_{xy}+$

(10) Goodness of Fit[15] Measure:

$$GOFM = \left\{ \sum_{I,J} [P(I,J)-P(I)P(J)]^2/[P(I)P(J)] \right\}^{1/2}$$

where P(I) and P(J) are the marginal distributions.

## 4. DATA ANALYSIS

LANDSAT Multispectral Scanner (MSS) digital data with spat
used in this study. Each scene is 185 km wide and 170 km in
stratocumulus, 8 cumulus, and 12 cirrus cloud scenes were ana
stratocumulus scenes and 7 of the cumulus scenes are shown in
the 12 cirrus scenes are shown in Kuo *et al*.[18]

Each of the 35 scenes is subdivided into 20 regions. Each
sample from the class of that scene, is 512 x 512 pixels (29
subregions, some contained no clouds. These clear subregions
database for this initial classification study.

discriminant function, chosen in a stepwise manner using the BM
for classification. Equal prior probabilities of belonging to
(stratocumulus, cumulus, cirrus) are assumed. The experiment
two holdout patterns, "scattered" and "contiguous."

## 5. RESULTS

The following summary table shows the classification accurac
(SC), 53 cumulus (Cu), and 76 cirrus (Ci) holdouts:

| | "Scattered" Pattern | | | "Conti |
|---|---|---|---|---|
| Actual \ Classified | Sc | Cu | Ci | Sc |
| Sc | 94 | 4 | 2 | 77 |
| Cu | 0 | 50 | 3 | 13 |
| Ci | 1 | 3 | 72 | 1 |

For the "scattered" holdout pattern, 94/100 of the stratocumulu
The 4/100 cases of stratocumulus classified as cumulus are regi
into cumulus. 50/53 cumulus scenes are correctly classified an
misclassified as stratocumulus. Finally, 72/76 cirrus are clas
one cirrus case classified as stratocumulus. The overall class
for the "scattered" pattern compared to 79.9% for the "contiguc
only 77/100 of the stratocumulus are classified correctly, 38/5
of the cirrus. Interestingly, cirrus have the overall highest
This is important because normally cirrus are difficult to dete
channel.

In the "scattered" holdout pattern, arbitrary regions from e
the classifier. In these cases, classification accuracy is ver
case has significantly lower accuracy because the holdout scene
ferent from the scenes used in the training data. This is a si
sets have been used to train the classifier. That is, the rang
each cloud class is larger than that of the 10 stratocumulus, 6
scenes used for training data. The 94.3% accuracy obtained usi
is a very encouraging indication that improvement of classifica
obtained simply by increasing the database.

The variables used in the final step of the classification a
Subscripts 1 and 2 refer to pixel distances d=1 and 2.

| Holdout Case | Variables |
|---|---|
| Scattered | $HOMOG_2$, $NOP_2$, $HOMOG_1$, $PROM_1$, $SHADE_2$ <br> $SHADEX_2$, $PROMX_2$, $PROMX_1$, $SHADEX_1$, P |
| Contiguous | $HOMOG_1$, $ENTROPY_2$, $CONTR_1$, $ENTROPY_1$, <br> $SHADE_1$, $SHADE_2$, $CORR_2$, $NOP_2$, $NOP_1$, |

## 6. CONCLUSION

Sengupta et al.[16] found the Number of Points ($NOP_1$) at d=1
classification of Brodatz[2] textures. This value represents th
constructed from nearest neighbor pixels. A large number of N
is a predominance of sharp gradients between MAX-MIN pairs. H
is found to be most useful in classification of cloud types.
stratus or cirrostratus which have small MAX-MIN differences s
homogeneity.

The 94% classification accuracy obtained for the "scattered
demonstrates that the MAX-MIN Cooccurrence Matrix method has g
classification. The method is computationally inexpensive and
visible channel. Use of directional texture measures allows o
field orientation.[17,18]

The present is a pilot study which merely demonstrates the
A larger database is required to improve the range of variabil
class. In addition, studies should be undertaken to include s
for land, water, ice, snow, mountains, cloud streets, cumuloni

## 7. ACKNOWLEDGMENTS

This investigation was conducted jointly under National Sci
No. ATM-8507918 and National Aeronautics and Space Administrat
Computations were made using the South Dakota School of Mines
computer. Appreciation is extended to Joie Robinson for typin

## 8. REFERENCES

1. BMDP Manual, pp. 519-537, University of Calif., Berkele
2. P. Brodatz, Textures, 112 pp., Dover, New York (1966).
3. J.T. Bunting and R.F. Fournier, "Tests of spectral clou
fine mode satellite data," Meteorology Division, AFGL-TR-80-01
Air Force Geophysics Lab (1980).
4. R.W. Connors and C.A. Harlow, "Toward a structural text
statistical methods," in Image Modeling, A. Rosenfeld, ed., Ac
(1981).
5. L.S. Davis, M. Clearman and J.K. Aggrawal, "An empirica
cooccurrence matrices," IEEE Trans. on Pattern Analysis and Ma
PAMI-3(3), 214-221 (1981).
6. R.M. Haralick, K.S. Shammugam and I. Dinstein, "Textura
classification," IEEE Trans. on Systems, Man and Cybernetics,
7. R.M. Haralick, "Statistical and structural approaches t
Joint Conf. Pattern Recognition, Kyoto, Japan, 45-69 (1978).
8. R.M. Hord, Remote Sensing, 362 pp., John Wiley and Sons
9. B. Julesz, "Visual pattern discrimination," IEEE Trans.
IT-8(2), 84-92 (1962).
10. O.R. Mitchell, C.R. Myers and W. Boyne, "A max-min meas
analysis," IEEE Trans. on Computers, 26(4), 408-414 (1977).
11. B.M. Mehtre, N.N. Murthy, B. Lipovsack and B. Chatterje
classification," Proc. Intnl. Geoscience and Remote Sensing Sy
Univ. of Mass., Amherst, 233-241 (1985).
12. J.A. Parikh, "A comparative study of cloud classificati
Sensing of Environ., 6, 67-81 (1977).
13. J.A. Parikh and A. Rosenfeld, "Automated segmentation a
meteorological satellite data," IEEE Trans. on Systems, Man an
736-743 (1978).
14. A. Rosenfeld and E.B. Troy, "Visual textural analysis,"
Feature Extraction and Selection in Pattern Recognition, IEEE
155-124 (1970).
15. A. Renyi, Probability Theory, 666 pp., North Holland/Am

# Clear sky estimation of surface albedo from digitized GC

James R. Foreman

Atmospheric Sciences Laboratory, Atmospheric Eff
Target Acquisition and Mobility Branch, White Sands Missile

ABSTRACT

A method is derived using digitised GOES east visual images
the Earth's surface. Atmospheric effects are accounted for wi
and Curran[1] which depend only on the solar zenith angle and wh
fit quantities derived from measurements. The albedos so four
ing satellite brightness counts, meteorological data, surface
astronomical computations, are in agreement with values cited

## 1. INTRODUCTION

A recurring problem in geophysical and atmospheric studies,
earth radiation budget and climate modelling studies, is the e
bedo, using imagery or upwelling radiance measurements from a
calibrated and accounting for effects of the atmosphere. The
dy shows promise of much greater accuracy in finding the albec

## 2. ESTIMATION OF SURFACE ALBEDO

### 2.1. Radiation balance of the Earth-atmosphere system

The broad-band, as defined by the spectral limits of the Ep
nometer (PSP), energy balance equation at the top of the Earth
written:

$$I_o = I_o \sum_{i=1}^{5} \alpha_i + I_R + I_s (1 - a_s) + I_s a_s \sum_{i=1}^{5} \alpha_i',$$

where: $I_o = S_o r^{-2} \cos \theta_o$ = the horizontal solar flux incident
atmosphere;

$S_o$ = normal incidence extraterrestrial solar flux at r = 1A

r = Earth-sun distance (astronomical units, AU);

$\theta_o$ = local solar zenith angle ($^o$);

$I_R$ = radiation reflected spaceward by the Earth-atmosphere

$\alpha_i$ = absorptivity of the i$^{th}$ atmospheric constituent for di
(i = 1 for water vapor, 2 for carbon dioxide, 3 for ozor
5 for suspended dust);

$\alpha_i'$ = absorptivity of the i$^{th}$ atmospheric constituent for sh
reflected upward by the Earth's surface, found from the
the $\alpha_i$'s, but with the relative optical air masses (ROAM

$I_s$ = insolation at the surface;

$a_s$ = surface albedo;

p = surface pressure (kPa); and

$p_o$ = 101.325kPa.

Dividing (1) by $I_o$ and denoting the fractional radiative qu
(e.g., $I_s/I_o = i_s$) yields

5 5

$$A_s(0,\theta_o) = 1 - \sum_{i=1}^{5} \alpha_i - i_s.$$

If the "slope function", $m_s(\theta_o)$, is defined as the partial der[illegible] spect to the surface albedo, then from (3),

$$m_s(\theta_o) = \frac{\partial A_s(a_s,\theta_o)}{\partial a_s} = i_s(1 - \sum_{i=1}^{5} \alpha_i')$$

which is independent of the surface albedo, $a_s$. Nack and Curr[illegible] provide relationships for (4) and (5) which depend only on the

$$A_s(0,\theta_o) = 0.0483 + 1.087 \times 10^{-5}\,\theta_o^2 - 2.219 \times 10^{-9}\,\theta_o^4 + 6.7[illegible]$$

and

$$m_s(\theta_o) = 0.7213 - 2.180 \times 10^{-9}\,\theta_o^4 - 4.941 \times 10^{-13}\,\theta_o^6.$$

Equations (4) and (5), then, make possible an experimental meth putation of the "intercept" and "slope" functions of Equations

First, the experimental value of $A_s(0,\theta_o)$ is computed from ( pyranometric measurements of $I_s$ and computed values of $I_o$ to fi ble clear sky insolation model to compute the $\alpha_i$ quantities. N ues are plotted against the corresponding N&C theoretical value If a significant difference is shown to exist between the set o and those obtained from (4), then a new dependence of $A_s(0,\theta_o)$ least-squares curve fitting. If no significant difference is f reason to suppose that any new relationship found from a limite better than (6). Next, a similar process is used to compare th values computed from (5) with the theoretical values from (7). cant difference between the two sets of values is found, a new is derived through least-squares curve fitting.

Once $A_s(0,\theta_o)$ and $m_s(\theta_o)$ are found, they may be substituted so that the surface albedo may be found from

$$a_s = [i_R - A_s(0,\theta_o)]/m_s(\theta_o).$$

## 2.2. Clear sky insolation model

After comparison of many clear sky insolation models (mostly the model of Hoyt[4] has been selected to compute the absorptivit[illegible] and (5). The following equations are presented without citatio[illegible] Hoyt[4].

For $H_2O$ vapor: $\alpha_1 = 0.11\,(u_{1p}m_w + 6.31 \times 10^{-4})^{0.3} - 0.0121;$

for $CO_2$: $\alpha_2 = 0.00235(126\,m_{kp} + 0.0129)^{0.26} - 7.5 \times 1[illegible]$

for $O_3$: $\alpha_3 = 0.045\,(u_3m_R + 8.34 \times 10^{-4})^{0.38} - 3.1 \times [illegible]$

$m_k = 1.0006/[\cos\theta_o + 0.150\ (93.885 - \theta_o)^{-1.253}]$; and

$m_R = 35\ (1224 \cos^2\theta_o + 1)^{-0.5}$.

Other quantities are:

$u_{1p}$ = the total water vapor column (cm or gm $cm^{-2}$) correct the spectral lines at each level by using (P + 5.3e)/1
P = atmospheric pressure at level (kPa);
e = water vapor partial pressure (kPa)
$\omega_o$ = the single scatter albedo of aerosols ($\cong$ 0.95);
$\beta$ = the Volz-Ångström turbidity coefficient; and
$g(\beta)$ = a function of $\beta$ from Table 2 in Hoyt[4]. From my owr

$g(\beta) = 0.947 - 1.044\ \beta + 0.00575/(\beta + 0.108)$.

## 3. APPLICATION OF THIS METHOD TO HAMPTON UNIVERSITY

### 3.1. Input data

February, 1982 has been chosen as the study period because my arrival in Hampton, Virginia $(\phi, \lambda) = (37.019^oN, 76.338^oW)$ which the surface albedo could be assumed to be approximately sists more than a couple of days in Hampton without cloud cov settled enough into my job to run a field study. 32 times we studies based on the following criteria: (1) Nominal Visual- (VISSR) scan time at Hampton; (2) sun at least $5^o$ above hori of zenith or $20^o$ of sun (based on sky condition observations between observations (this final criterion is relaxed on Febr date on which local turbidity observations have been made). cut further to 23 because of difficulties in finding the Ham in seven low solar elevation cases, and in tape reading pari

Values for the normal incidence extraterrestrial solar fl Hickey et al.[5] for fifteen days in the period January 29 throu case study times have been obtained through linear interpola

Surface (temperature, dew point and station pressure) and points, winds and geopotential heights at pressure levels) m obtained from the NOAA National Climatic Center Environmenta ces (NOAA/NCC/EDIS), Asheville, NC, for 21 surface and four ton. The upper level data have been used to determine the wa This quantity, and the surface station pressures, are adjust lation.[6] The upper level data are interpolated to Hampton by

$$Q = a + bL + cE + dLE$$

where Q is the interpolated quantity, L and E are the VISSR spatial analyses in this study have been done using GOES ima d are exact fit coefficients. This quantity is then evaluat site values of L and E. The surface pressure at Hampton Uni age of the pressures at two nearby stations (Langley AFB and square of the distance from the Hampton site.

Dobson spectrophotometer measurements of the total ozone for four nearby stations from the Canadian Atmospheric Envir Data Centre. Spatial interpolation is from (18) and time in

One minute integrated totals of the insolation have been made throughout the study period. The instrument is an Eppley PSP wi clear glass dome. Four-minute totals are obtained from these, i the high resolution of the satellite solar radiation study as ha short integrating period, however, limits the significant figure some uncertainty has been introduced into measurements of $I_s$.

Visual images of the highest (approximately 0.8 x 1km at nadi tained for all 32 original cases in the On-line Data Ingest Sys University of Wisconsin Space Sciences Engineering Center (UW/SS ronmental Satellite Services Data and Information Service (NOAA/ calibrated using the method of Norton et al[7] with histograms pro of the UW/SSEC. Because of problems in navigating the images ( mat navigation parameters), the images are registered manually sitions. Once the pixel containing the Hampton site has been fou array, centered on this pixel, is extracted and a weighted avera brightness counts is made. The weights are proportional to the tance from the central pixel and an arbitrary large but finite central pixel. This weighting accounts for effects of sub-pixel adjacency effects. Finally, to get $I_R$, the non-isotropic refle counted for using the bi-directional reflectance model of Raschk site includes both land and water, both land and water reflecta

3.2 Results

3.2.1. The N&C "intercept function", $A_s(0,\theta_o)$. This function is case, from experimental data and Equation (4) along with the cl This function is also estimated from Equation (6). A scattergra these two sets of estimates, shows ample agreement (correlation 0.0054 and mean square error = $2.85 \times 10^{-4}$). Figure 1 shows bo points) and theoretical (smooth curve) values of the "intercept the solar zenith angle, $\theta_o$. It can be seen that these values a that this agreement extends across the range of solar zenith an test of the hypothesis, that $A_{s(exp.)}(0,\theta_o) = \beta_o + \beta_1 A_{s(th.)}(0,$ coefficients $\beta_o = 0$ and $\beta_1 = 1$, could not reject this hypothesi said that $A_s(0,\theta_o)$ can be just as well estimated from Equation a least-squares fitting of $A_s$ versus $\theta_o$ with only 23 cases.

3.2.2. The N&C "slope function", $m_s(\theta_o)$. Equation (5), along w the absorptivities and the experimental data, are used to estima also used to estimate this function. A scattergram (not shown) timates, though showing a strong correlation ( = 0.995), also s theoretical over the experimental set (mean bias error = -0.112 0.0145). In fact, there is not one value in the theoretical se experimental counterpart by at least 0.059. Thus, it has been form any hypothesis test on whether the theoretical set differs A new formula, made from least squares curve fitting, replaces

$$m_s(\theta_o) = 0.6270 - 1.345 \times 10^{-9}\,\theta_o^4 - 8.403 \times 10^{-13}\,\theta_o^6.$$

Figure 2 shows the experimental (data points) and both of the t (7) and (19) (smooth curves), as functions of the solar zenith a results produce a different "slope function" than that from N&C

3.2.3. Surface Albedo. Equation (8) is solved for the surface

has been derived from a least-squares linear fit and is plotte
$a_s$ values is used to test the hypothesis that $\hat{a}_s = \bar{a}_s$ ( = ense
The F-test reveals that this hypothesis can not be rejected ar
cepted as the surface albedo, independent of the solar zenith
out, however, that a positive dependence of the surface albedc
has been found by many scientists for land and water surfaces.
agreement with many findings for semi-urban snow-free sites wi
binson and Kukla[10]).

## 4. CONCLUSIONS

The problems of finding the albedo of a point on the surfac
for atmospheric effects and using a satellite radiometer of qu
been sidestepped by using a model of atmospheric effedts which
zenith angle. The two main relationships in this model (Equat
may be reparameterized if a set of values derived from them de
set of values derived from meteorological data and a clear sky
fectively "recalibrates" the GOES east visual sensors. The re
very reasonable and in agreement with published values for sin
ter conditions. This is a great improvement in accuracy over
visual data.

This topic is dealt with in greater detail in Foreman[9].

## 5. REFERENCES


1. M.L. Nack and R.J. Curran, NASA TM 78057: Transformati
face-Atmosphere Albedo and Irradiance, and Their Spectral and
NASA Goddard Space Flight Center, Greenbelt, MD (1978).
2. R.E. Bird and R.L. Hulstrom, SERI/TR-335-344: Direct I
Research Institute, Golden, CO (1980).
3. ----- and -----, SERI/TR-642-761: A Simplified Clear S
fuse Insolation on Horizontal Surfaces, 38pp, Solar Energy Re
(1981).
4. D.V. Hoyt, "A model for the calculation of solar global
21, 27-35 (1978) (See, also, Erratum in Ibid., 25, pp. 193 an
5. J.R. Hickey, B.M. Alton, F.J. Griffin, H. Jacobowitz, P
E.A. Smith and T.H. Vonder Haar, "Extraterrestrial solar irra
one-half years of measurements from Nimbus-7," Solar Energy, 
6. G.J. Haltiner, Numerical Weather Prediction, 317pp, Joh
don, Sydney, Toronto (1971).
7. C.C. Norton, F.R. Mosher, B. Hinton, D.W. Martin, D. Sa
for calculating desert aerosol turbidity over the oceans from
data," J. Appl. Meteor., 19, 633-644 (1980).
8. E. Raschke, T.H. Vonder Haar, M. Pasternak and W.R. Ban
diation Balance of the Earth-Atmosphere System from Nimbus 3
National Aeronautics and Space Administration, Washington, DC
9. J.R. Foreman, Estimation of Surface Albedo and Light Ab
sols under Clear Skies from Digitised GOES-East Visual Images
Michigan, 217pp, (1986).
10. D.A. Robinson and G. Kukla, "Albedo of a dissipating s
Meteor., 23, 1626-1634 (1984).

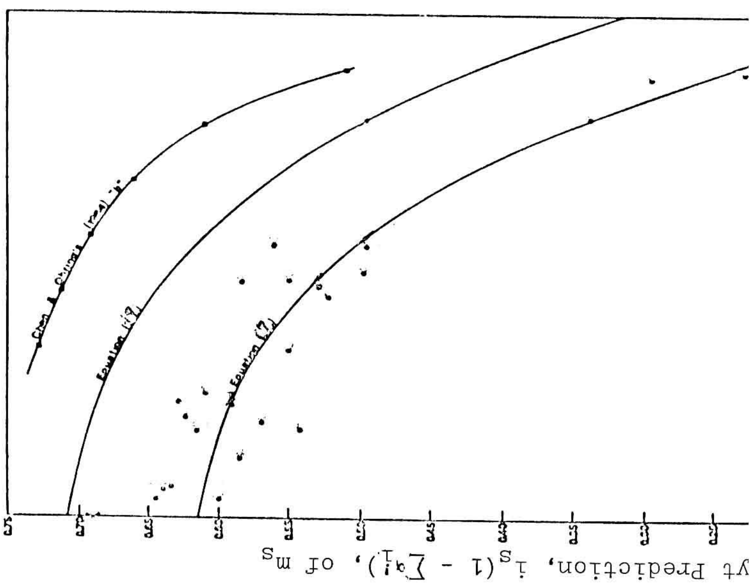
yt Prediction, $i_s(1 - \sum q_i)$, of $m_s$